

Additively Manufactured Flexible On-Package Phased Antenna Arrays With Integrated Microfluidic Cooling Channels for 5G/mmWave System-on-Package Designs

Kexin Hu¹, Graduate Student Member, IEEE, Theodore W. Callis¹, Student Member, IEEE, and Manos M. Tentzeris¹, Fellow, IEEE

Abstract—A fully additively manufactured flexible reconfigurable on-package antenna array with an integrated microfluidic cooling channel is introduced. The proposed design is a multilayer topology that can be easily embedded within flexible hybrid electronics (FHE) packages, utilizing 3-D printing and inkjet printing technologies. A novel 2.5-D ultra-wideband (UWB) antenna array operating from 24 to 40 GHz was designed and fabricated, and a beamformer IC was integrated with the inkjet-printed antenna array through room-temperature conductive silver paste as a proof-of-concept demonstration. The microfluidic channel attached to the on-package antenna array was stereolithography (SLA) printed using Flex80A resin from Formlabs. The measured radiation pattern of the integrated package showed a 10.09 dBi maximum realized gain with beam steering range from -37° to 37° . The temperature change of the IC was also monitored, and the results showed a 10 °F drop in 5 min. This low-cost and low-temperature fabrication process using additive manufacturing can be effectively applied to many 3-D printed materials that are sensitive to thermal treatment, as to next-generation multichip module (MCM) integration on flexible materials for 5G/mmWave system-on-package designs.

Index Terms—3-D printing, 5G, additive manufacturing, flexible electronics, inkjet printing, millimeter-wave devices, phased array, ultra-wideband (UWB) antennas.

I. INTRODUCTION

THE emerging 5G and mmWave technologies have enabled higher data speeds and wideband operations bringing about the development of next-generation Internet of Things, large-scale smart cities, and wearable electronics for health monitoring. With the demand for beamforming to overcome high path loss in mmWave frequencies, flexible phased arrays become significant because they feature adaptive beam steerability and deployable structures for various platforms. Additive manufacturing technologies have been very popular in flexible hybrid electronics (FHE) designs because of flexible

Manuscript received 28 February 2023; revised 10 April 2023; accepted 15 April 2023. Date of publication 1 May 2023; date of current version 7 June 2023. This work was supported by the Army Research Laboratory with SEMI-FlexTech and was accomplished under Cooperative under Agreement W911NF-19-2-0345. (Corresponding author: Kexin Hu.)

The authors are with the Georgia Institute of Technology, School of Electrical and Computer Engineering, Atlanta, GA 30332 USA (e-mail: khu63@gatech.edu).

This article was presented at the IEEE MTT-S International Microwave Symposium (IMS 2023), San Diego, CA, USA, June 11–16, 2023.

Color versions of one or more figures in this letter are available at <https://doi.org/10.1109/LMWT.2023.3268237>.

Digital Object Identifier 10.1109/LMWT.2023.3268237

2771-957X © 2023 IEEE. Personal use is permitted, but republication/redistribution requires IEEE permission. See <https://www.ieee.org/publications/rights/index.html> for more information.

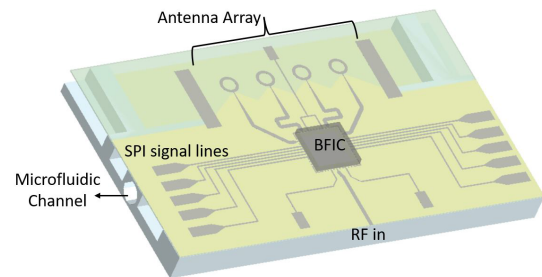


Fig. 1. Schematic of a proof-of-concept flexible additively manufactured on-package phased array with the integrated microfluidic cooling channel.

materials that can be easily inkjet printed or 3-D printed in customized structures with extremely low cost and less waste [1]. However, there are many challenges in the implementation of an additively manufactured multichip module (MCM) on flexible substrates. Most 3-D printed flexible materials have relatively low melting temperatures [2]. The resulting deformation of substrates undergoing the thermal process may deteriorate the performance of the electronics. The metallization process on flexible substrates usually utilizes printable conductive ink that is not solderable, which makes it difficult to apply traditional assembly processes. Past research utilized commercially available flexible polyethylene terephthalate (PET) or Kapton sheets as substrates [3], but these ready-to-use materials largely limit their applications in customized packaging designs with complicated structures. Conductive epoxy was used to attach components onto a flexible substrate, but this becomes challenging for mmWave ICs due to the smaller pad and pin size. Finally, with flexible polymer substrates, heat dissipation of the IC may become an issue because the thermal conductivity of these materials is poor compared with traditional rigid copper substrates like Rogers [4].

To address these challenges, this letter introduces an additively manufactured solution to mmWave IC integration with flexible substrates, utilizing a novel inkjet-printed 2.5-D ultra-wideband (UWB) antenna array on a 3-D printed polypropylene (PP) substrate, with a 3-D printed microfluidic channel for IC cooling, as shown in Fig. 1. 3-D printed substrates provide more freedom in design customization and can support quick turnaround time for multiple iterations [1]. The UWB 5G/mmWave antenna array was inkjet printed with silver nanoparticle (SNP) ink with operational bandwidth covering 24–40 GHz. A beamformer IC was successfully attached to the inkjet-printed antenna array to achieve broadside beamsteering

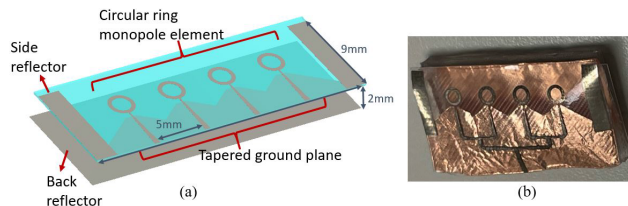


Fig. 2. 2.5-D UWB antenna array. (a) Schematic of the UWB antenna array design. (b) Fabricated UWB antenna array prototype.

from -37° to 37° , while the temperature of the IC can be reduced from 108°F to 98°F in 5 min through microfluidic cooling with water. The key innovation in this design is the customized multilayer and multifunction packaging topology enabled by a low-temperature fabrication and assembly process. The reported 5G/mmWave packaging module using additive manufacturing can be widely used for future multichip integration in flexible system-on-package designs.

II. ADDITIVELY MANUFACTURED 2.5-D PHASED ANTENNA ARRAY

A. Design of a 2.5-D Ultrawideband Antenna Array

Conventional UWB antenna elements like horn antennas and Vivaldi antennas are relatively bulky, and UWB antenna arrays using monopole elements only demonstrate an endfire radiation pattern that features a radiation peak parallel to the substrate plane [5]. These designs are challenging in compact integration when broadside radiation is preferred, for example, wearable devices require good flexibility and isolated radiation from the human body. This letter presents a novel UWB antenna array operating from 24 to 40 GHz to cover the entire 5G mmWave frequency band. The antenna array is a 2.5-D structure that includes a planar circular monopole antenna array, a back reflector with 2 mm spacing at the bottom, and side reflectors with 4 mm spacing from the antenna array, enabling broadside radiation with enhanced beamforming characteristics and lower sidelobe level, as shown in Fig. 2. The spacing between reflectors and the monopole array would affect the impedance matching and maximum gain of the array, which was optimized in CST Microwave Studio. The back reflector can be realized using 3-D printing to create customized multilayer structures. The tapered feedlines and ground plane help to adjust the impedance matching to $50\ \Omega$ and achieve UWB operation.

III. FABRICATION OF ON-PACKAGE PHASED ARRAY

The substrate of the designed antenna array is 3-D printed PP from an fused deposition modeling (FDM) printer (Ultimaker S3) that has been proven to have very low RF loss up to 40 GHz, comparable to other commercial substrates for RF applications [6]. The substrate thickness is 0.2 mm. The surface was pretreated, and SU8 buffer layers were inkjet printed to improve smoothness for better adhesion of SNP ink [7]. The antenna array and the IC footprint were then inkjet printed with SNP ink (Suntronic, EMD5730) from an inkjet printer (Fuji Dimatix DMP 2850). Six layers of SNP ink were printed in total from a Samba printing cartridge (Fuji Dimatix) to ensure adequate metallization thickness and good ink coverage. UV sintering instead of thermal sintering was used to prevent severe warpage from the substrates, due to different thermal expansion coefficients between multiple deposited layers. First, the inkjet-printed silver antenna was dried at 90°C for 10 min, and then 30 pulses of UV light

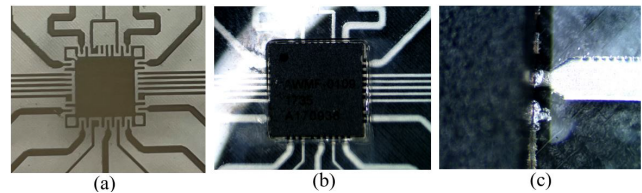


Fig. 3. Inkjet printed IC footprint and IC alignment. (a) Inkjet printed IC footprint on a 3-D printed PP substrate. (b) IC placement within a PET stencil. (c) Alignment of the pins after epoxy curing.

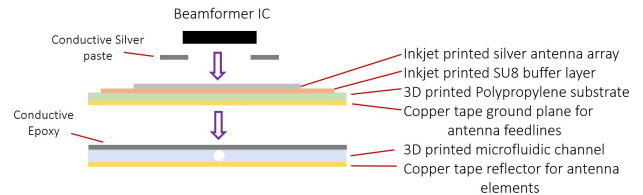


Fig. 4. Cross-sectional schematic of the fabrication process of the proof-of-concept module.

with 830 J were applied from a Xenon X-1100. The whole sintering process lasted less than 30 s and there was no obvious mechanical deformation on the substrate. The flatness of the substrate after sintering was critical for the precise alignment of the IC and accurate measurements of phased array performance.

The attachment of the beamformer IC was the most important step in the fabrication process. To demonstrate the successful integration and functionality of the package, the Anokiwave chip AWMF-0109 in a quad flat no-lead (QFN)-48 package was used for testing, which operates from 27.5 to 30 GHz, covering the center frequency of the designed wideband antenna array. Conductive epoxy is most commonly used in attaching components onto thermal sensitive substrates, but the epoxy deposition cannot be effectively constrained only within the pads area, and therefore a small misalignment of the IC will cause a short between neighboring pins. Also, the IC detaches easily when the epoxy dries up. Another potential solution is the use of low-temperature anisotropic conductive adhesive (ACA material). It is difficult to achieve solid connections on soft and flexible substrate material because FDM printed materials have an uneven surface pattern. However, ACA material has been proved to be a very reliable and mechanically strong adhesive material [8], [9], which can be used to enhance the attachment of IC in this work.

Therefore, the assembly process used in this work leverages the pros and cons of the aforementioned methods to ensure very good alignment and attachment of the IC. After inkjet printing and sintering of the antenna pattern, vias were implemented by drilling holes 0.2 mm in diameter and filling them with silver conductive paste. For ground plane metallization, it is feasible to inkjet print SNP ink, but the copper tape was used to conduct fast iterations of fabrication and testing for IC attachment. A stencil was fabricated on a transparent PET sheet from a laser cutter with the exact size of the IC (6×6 mm). The transparent PET stencil allows for thorough verification of the alignment of each pin even after placing the IC (Fig. 3). A conductive adhesive epoxy (MG Chemicals 8331D) was carefully applied to each pad of the inkjet-printed IC footprint, and the stencil was put on top of the IC footprint according to the reference markers that were inkjet printed along with the footprint of the IC at four corners. Then, the IC was accurately placed within the stencil. The pressure was applied uniformly on top of the IC until

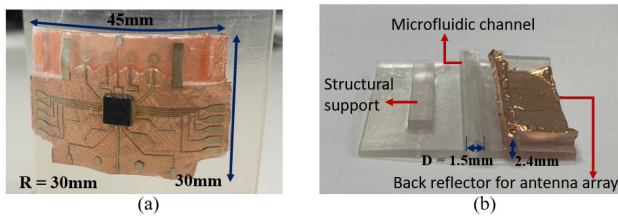


Fig. 5. Proof-of-concept additively manufactured phased array prototype with an integrated microfluidic cooling channel. (a) Top view of the flexible on-package phased antenna array bent over a curved surface with a 30-mm radius. (b) Side view of the SLA printed microfluidic channel module.

the paste was fully cured at room temperature to ensure a solid electrical connection. The wires were attached to the dc pads for serial peripheral interface (SPI) connection using the same conductive epoxy. Finally, an ACA material (Creative Material, 129-47) was used to seal the corners and edges of the IC and cured at 95 °C for 30 min, to enhance mechanical connection. Fig. 4 shows the cross-sectional schematic of the proposed fabrication process.

The fabricated on-package phased array prototype is shown in Fig. 5(a). The integrated package with a 3-D printed microfluidic channel can be conformally bent over a curved surface with a 30-mm radius, demonstrating excellent flexibility and good mechanical strength. The inkjet printing process used in the work has featured very good reliability in both electrical and mechanical performance over 10 000 times of cyclic bending tests [7] as well as in preliminary single-embedded IC structures for radii of curvature down to 30 mm. Additional tests for multichip topologies following the same reliability tests will be performed and presented at IMS. The proposed fabrication and assembly process can be easily adapted to many other 3-D printed flexible materials, enabling wider applications of future 5G/mmW system-on-package materials.

IV. ADDITIVELY MANUFACTURED MICROFLUIDIC COOLING CHANNEL

The motivation for the design of a microfluidic cooling channel stems from the poor thermal conductivity of common 3-D printed polymer materials. A simple cylinder cooling pipe is presented as a proof-of-concept demonstration for additive manufacturing capabilities and in-package integrability. The design of the fluid channel and the accompanying antenna array module was modeled in Solidworks. The fluid channel was embedded in the module by extruding a 1.5-mm diameter cylindrical pipe with 0.2-mm-thick walls that runs below the beamformer IC as shown in Fig. 5(b). A back reflector metalized with copper tape was also placed below the circular ring monopole elements, and a 3-D printed structural support rod was added separately from the microfluidic channel to facilitate measurements without affecting heat dissipation and flexibility of the module. A 1.5-mm diameter was used to flow the maximum amount of water to achieve greater cooling while also adhering to the 3-D print tolerances and providing good flexibility. Printing channels with greater diameters resulted in channels that were too fragile.

The microfluidic channel and associated module were 3-D printed using an stereolithography (SLA) printer (Form3, Formlabs). No internal support structures within the channels were needed during the print so that the channel walls could remain smooth. The material used to print the channel and module was Flexible 80 A, a flexible and durable 3-D printing material made by Formlabs. After being printed, the module

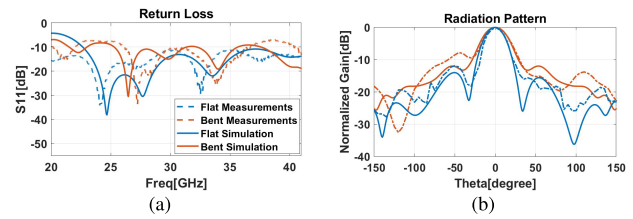


Fig. 6. (a) Comparison of simulated and measured S11 values and (b) radiation pattern [H-plane] for the proof-of-concept prototype in flat and bent with a radius of 30 mm configurations.

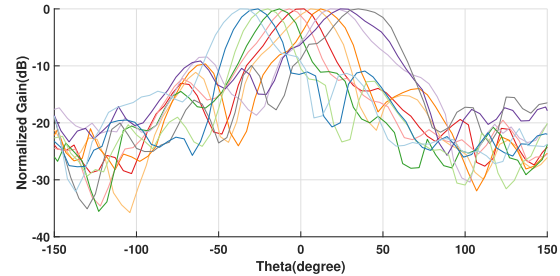


Fig. 7. Beam steering measurement results of the fabricated phased array module prototype with an integrated microfluidic channel.

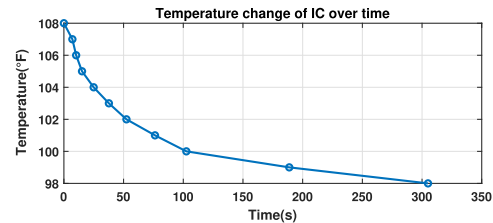


Fig. 8. Cooling of the IC over time through the use of a microfluidic channel.

was washed in IPA for 20 min and cured under UV light for 10 min. The external support structures were cut off from the printed module. The antenna array was attached to the module with conductive epoxy.

V. RESULTS AND DISCUSSION

The integrated phased array module was measured in an anechoic chamber. The S11 response and the radiation pattern at 30 GHz of the fabricated antenna array were measured under both flat and bent conditions, where a cylinder with a 30-mm radius was used. 30-mm bending radius is selected as an example similar to the average size of a human wrist, to satisfy flexibility requirements for most wearable applications. As shown in Fig. 6, the measurement results agree well with the simulation. Comparing the results under flat and bent conditions, bending the antenna module can shift the operational frequencies and slightly increase the beamwidth and sidelobe level, mainly because of the change in impedance matching and element spacing. The overall performance of the antenna under bending is still acceptable. The measurement results of beamsteering at 30 GHz under flat condition is shown in Fig. 7. The inkjet-printed phased array achieved -37° to 37° beamsteering without showing grating lobes, and a maximum sidelobe level of -8.45 dB. The maximum realized gain was 10.09 dBi and gain degradation was less than 4 dB between steering beams. The asymmetry between beamwidth can be caused by the slight warpage and bending of the soft antenna substrate.

Measurements of the fluid channel were set up by connecting a Yanmis 12 V peristaltic pump to the fluid channel and a room temperature (70 °F) water supply. Water was pumped through the channel at 1.45 mL/s. The temperature

was measured by a Kaiweets HT 118A thermocouple fixed atop the IC. The starting temperature of the IC was 108 °F when the maximum power was consumed by the IC. The steady-state temperature value was reached after around 5 min at 98 °F, as shown in Fig. 8. The calculated heat dissipation is 1.052 W [10], assuming that the thermal conductivity value of Flexible 80 A is 0.283 W/m · K, provided by Formlabs, and that heat is transferred through a rectangular cross-sectional area. The heat dissipation in this design is mainly limited by the low thermal conductivity of polymer substrates. However, the additively manufactured array module with integrated cooling function has enabled high flexibility and significantly reduced the size and weight compared with traditional designs on printed circuit board (PCB) substrates with microfluidic cooling [11], [12]. Furthermore, recent research shows possible modifications on 3-D printed materials to improve thermal performance [13], and therefore, it is expected in the future that better cooling performance can be achieved using the proposed packaging topology.

VI. CONCLUSION

This letter presents the first fully additively manufactured flexible on-package phased array with an integrated microfluidic channel for IC cooling. The 2.5-D UWB miniaturized antenna array covering 24–40 GHz can be used for a variety of broadband 5G/mmW applications. The attached beamformer IC shows a reliable electrical and mechanical connection that is sustainable for practical bending radii in flexible wearable applications. Cooling by the microfluidic channel suggests sufficient mitigation of IC temperatures. Last, but not least, the proposed low-temperature IC alignment/assembly process would set the foundation for next-generation highly complex FHE and flexible MCM and phased array on-package modules using 3-D/inkjet printing for wearable, smart skin, and implantable (using biocompatible substrates, such as PP) applications.

ACKNOWLEDGMENT

The views and conclusions contained in this document are those of the authors and should not be interpreted as representing the official policies, either expressed or implied, of the Army Research Laboratory or the U.S. Government or SEMI. The U.S. Government is authorized to reproduce and distribute reprints for Government purposes notwithstanding any copyright notation herein.

REFERENCES

- [1] B. K. Tehrani, R. A. Bahr, W. Su, B. S. Cook, and M. M. Tentzeris, "E-band characterization of 3D-printed dielectrics for fully-printed millimeter-wave wireless system packaging," in *IEEE MTT-S Int. Microw. Symp. Dig.*, Jun. 2017, pp. 1756–1759.
- [2] J. L. Storck, G. Ehrmann, J. Uthoff, E. Diestelhorst, T. Blachowicz, and A. Ehrmann, "Investigating inexpensive polymeric 3D printed materials under extreme thermal conditions," *Mater. Futures*, vol. 1, no. 1, Feb. 2022, Art. no. 015001.
- [3] W. T. Li, Y. Q. Hei, P. M. Grubb, X.-W. Shi, and R. T. Chen, "Inkjet printing of wideband stacked microstrip patch array antenna on ultrathin flexible substrates," *IEEE Trans. Compon., Packag., Manuf. Technol.*, vol. 8, no. 9, pp. 1695–1701, Sep. 2018.
- [4] C. Shemelya et al., "Anisotropy of thermal conductivity in 3D printed polymer matrix composites for space based cube satellites," *Additive Manuf.*, vol. 16, pp. 186–196, Aug. 2017.
- [5] T. H. Lin et al., "Broadband and miniaturized antenna-in-package (AiP) design for 5G applications," *IEEE Antennas Wireless Propag. Lett.*, vol. 19, no. 11, pp. 1963–1967, May 2020.
- [6] K. Hu, Y. Zhou, S. K. Sitaraman, and M. M. Tentzeris, "Additively manufactured flexible material characterization and on-demand 'smart' packaging topologies for 5G/mmWave wearable applications," in *Proc. IEEE 73rd Electron. Compon. Technol. Conf. (ECTC)*, May 2023.
- [7] Y. Zhou, K. Hu, M. M. Tentzeris, and S. K. Sitaraman, "Mechanical and Ka-band electrical reliability testing of interconnects in 5G wearable system-on-package designs under bending," in *Proc. IEEE 72nd Electron. Compon. Technol. Conf. (ECTC)*, May 2022, pp. 914–923.
- [8] R. Al-Haidari et al., "Evaluation of an anisotropic conductive epoxy for interconnecting highly stretchable conductors to various surfaces," in *Proc. IEEE 72nd Electron. Compon. Technol. Conf. (ECTC)*, May 2022, pp. 1422–1429.
- [9] A. Stennermann et al., "Robustness and reliability of novel anisotropic conductive epoxy for stretchable wearable electronics," in *Proc. IEEE 72nd Electron. Compon. Technol. Conf. (ECTC)*, May 2022, pp. 762–768.
- [10] J. Welty, G. Rorrer, and D. Foster, *Fundamentals of Momentum, Heat, and Mass Transfer*, 6th ed. Hoboken, NJ, USA: Wiley, 2018.
- [11] K. Temir and O. F. Yalim, "A method of electro-mechanical packaging with embedded cooling to design fully-functional core structures for scalable active phased array radars," in *Proc. IEEE Int. Symp. Phased Array Syst. Technol. (PAST)*, Oct. 2019, pp. 1–3.
- [12] T.-W. Wei et al., "Demonstration of package level 3D-printed direct jet impingement cooling applied to high power, large die applications," in *Proc. IEEE 70th Electron. Compon. Technol. Conf. (ECTC)*, Jun. 2020, pp. 1422–1429.
- [13] M. Smith et al., "Maximizing the performance of a 3D printed heat sink by accounting for anisotropic thermal conductivity during filament deposition," in *Proc. 18th IEEE Intersociety Conf. Thermal Thermomechanical Phenomena Electron. Syst. (ITherm)*, May 2019, pp. 626–632.